Computational Mechanics (2022) 70:993–1011
https://doi.org/10.1007/s00466-022-02196-5

ORIGINAL PAPER

Efficient acoustic topology optimization with the Multifrequency Quasi-Static Ritz vector (MQSRV) method

Myung Shin[1] · **Gil Ho Yoon**[1]

Received: 16 January 2022 / Accepted: 26 May 2022 / Published online: 18 June 2022

Abstract
This research develops a new acoustic topology optimization scheme with a model order reduction called the Multifrequency Quasi Static Ritz Vector (MQSRV) method which effectively reduces the size of the system matrix for the calculating responses as well as sensitivity values in frequency domain. Computing the accurate acoustic responses and sensitivity values with the finite element (FE) method usually requires a significant amount of computational resources. For an efficient optimization, this research adopts recent developments in computational model order reduction approach having successfully exploited advanced mathematical development for calculating accurate solutions of partial differential equation. Among model order reduction schemes, the present study uses the MQSRV method which calculates the Ritz vector bases at multiple frequencies to minimize the amplitude of sound pressure in objective domain. Through several design examples, the efficiency and reliability of the MQSRV method for the acoustic topology optimization are verified.

Keywords Model order reduction · Topology optimization · Ritz vector · Acoustic

1 Introduction

This research develops a new acoustic topology optimization scheme with the Multifrequency Quasi Static Ritz Vector (MQSRV) method calculating the Ritz vector bases at multiple frequencies. Computing the accurate acoustic responses and sensitivity values with the finite element (FE) method usually requires a significant amount of computation time. For an efficient optimization, the model order reduction allowing us to compute the responses and sensitivity values efficiently has been widely adopted. Among various model order reduction schemes, the present study adopts the MQSRV method calculating the Ritz vector bases at multiple frequencies. Through several design examples, the efficiency and reliability of the MQSRV method for the acoustic topology optimization are verified.

Several relevant researches for acoustic topology optimization have been carried out. In the framework of finite element method and topology optimization, several researches for acoustic or vibration topology optimization can be found [4,10,11,16,17,19,20,24,26,34]. Before the developments of acoustic related problems, many relevant researches exist for structural vibration problems (See [16,17,19,26] and references therein). With the help of the topology optimization for vibrating structure, acoustic topology optimization also has been researched. In [4], the noise reduction by topology optimization was pursued with Helmholtz equation. In [34], the acoustic-structure interaction phenomena was considered in topology optimization. In [11], acoustic topology optimization was applied for noise barrier design. In [10], a floating projection topology optimization method based on the mixed displacement/pressure finite element formulation was proposed. Besides there are still many research for for acoustic topology optimization.

The model order reduction scheme has been researched in order to incorporated with the acoustic simulation and the acoustic topology optimization. As acoustic topology optimization usually requires a lot of computation time compared with the topology optimization for static or quasi-static problem, the model order reduction schemes which reduce the size of system matrix are regarded as a remedy for efficient optimization. To our best knowledge, several model order reduction schemes have been proposed (See the references [1–3,5–9,12–15,18,21–23,25,27–33,35–37]). In [32], it is shown that it is possible to use the model order

✉ Gil Ho Yoon
ghy@hanyang.ac.kr ; gilho.yoon@gmail.com

[1] School of Mechanical Engineering, Hanyang University, Seoul, South Korea

reduction in topology optimization and several model reduction schemes were used to reduce the size of the dynamic stiffness matrix, to calculate the dynamic responses and sensitivity values with adequate efficiency and accuracy for topology optimization in frequency domain. In [12], the multi-substructure multi-frequency quasi-static Ritz vector (MMQSRV) method generating the reduction bases at multiple substructures was proposed for an efficient topology optimization scheme. In [30], the reduced multiscale model for nonlinear macroscopic structural was presented using Proper Orthogonal Decomposition (POD). In [37], the effectiveness of the mode displacement method and the mode acceleration method for time-domain response problems was investigated to reduce computational cost for the dynamic response topology optimization problems. In [2], reduced order model (ROM)-based structure topology optimization algorithm for that enables a fast design process was presented. In [8], model order reduction techniques to optimal design to reduce the transient analysis time was applied for the application of MEMS design. In [36], interpolated as surrogate models was used for an optimization procedure. In [14], a systematic comparative study of some typical and potential model order reduction for solving the broad band frequency response optimization problems is provided, including the Quasi-Static Ritz Vector (QSRV), the Padé expansion and the second-order Krylov subspace method. In [18], the computational efficiency was further improved in each optimization iteration by employing a reduced order model when designing material micro-structures by using isogeometric analysis and parameterized level set method. In short, many relevant researches have tried to use the idea of the various model order reduction scheme in optimization.

The present study develops a new accelerated acoustic topology optimization scheme to minimize the amplitude of sound pressure in the objective domain with the MQSRV method. Compared with the existing model order reduction schemes, the MQSRV method computes the Ritz vectors at multiple center frequencies. The idea with benefit behind the MQSRV method are that Ritz vectors at one frequency can be alternative or better bases at different frequencies. Therefore, by combining the bases generated at multiple frequencies, a set of Ritz vectors which is effective for a wide range of frequency domain can be generated. For example, the inversions of the dynamic stiffness matrix, i.e., Stiffnessmatrix $-\ {\omega_c}^2$Mass matrix (ω_c: center frequency), is computed and the bases at a center frequency can be combined with the bases at a different center frequency [12,33,35]. This approach becomes effective for harmonic analysis whose responses should be computed at a wide frequency domain or separated frequency domains. Thus, in the present study, the acoustic topology optimization problems with responses at separated frequency domains are also solved to show the effectiveness of the present study.

The paper is organized as follows. Sect. 2 provides some backgrounds to the topology optimization and the MQSRV method to reduce the system size in acoustic system. In Sect. 3, several optimization studies in 2D and 3D are presented. Sect. 4 provides the conclusions and suggestions for future research topics.

2 Acoustic optimization formulation

2.1 Finite element procedure for linear acoustics

To analyze acoustic propagation in frequency domain, the following Helmholtz equation is formulated and numerically solved:

$$\nabla \cdot (\rho^{-1} \nabla p) - \omega^2 \kappa^{-1} p = 0 \text{ on } \Omega \ \ (\kappa = \rho c^2) \tag{1}$$

where p, ρ, κ, c and ω are the pressure in the analysis domain Ω, the local density, the bulk modulus, the local speed of sound, and the angular frequency of sound wave, respectively. In addition, the following boundary conditions are imposed.

$$\text{Sound pressure condition} : p = p_{\text{source}} \tag{2}$$

$$\text{Hard wall B.C} : \mathbf{n} \cdot \nabla p = 0 \tag{3}$$

$$\text{Sommerfeld B.C} : \mathbf{n} \cdot \nabla p + i \cdot \frac{\omega}{c} \cdot p = 2i \cdot \frac{\omega}{c} \cdot p_{\text{in}} \tag{4}$$

where the sound source and the incoming input pressure are denoted by p_{source} and p_{in}, respectively. The outward unit normal vector is denoted by $\mathbf{n}$. In the framework of the acoustic finite element procedure, the above Helmholtz equations is discretized as follows:

$$\mathbf{SP} = (\mathbf{K} - \omega^2 \mathbf{M} + i\omega \mathbf{F}^{\text{radiation}})\mathbf{P} = \mathbf{F} \tag{5}$$

where the the system matrix and sound pressure vector are denoted by $\mathbf{S}$ and $\mathbf{P}$, respectively. The stiffness matrix and the mass matrix are denoted by $\mathbf{K}$ and $\mathbf{M}$, respectively. The radiation matrix and the boundary term, i.e., $\mathbf{F}^{\text{radiation}}$ and $\mathbf{F}$ for Sommerfeld boundary condition and the boundary conditions, are formulated and included. In the framework of the finite element method, the above matrices and the vectors are formulated as follows:

$$\mathbf{K} = \mathop{\mathbf{A}}_{e=1}^{\text{NE}}{}_{\text{m}} \mathbf{k}_e, \ \mathbf{M} = \mathop{\mathbf{A}}_{e=1}^{\text{NE}}{}_{\text{m}} \mathbf{m}_e,$$

$$\mathbf{F}^{\text{radiation}} = \mathop{\mathbf{A}}_{e=1}^{\text{NE}}{}_{\text{v}} \mathbf{f}_e^{\text{radiation}}$$

$$\mathbf{k}_e = \rho_e^{-1} \int_{\Omega_e} \mathbf{B}^{\text{T}} \mathbf{B} \, \text{d}\Omega$$

$$\mathbf{m}_e = \kappa_e^{-1} \int_{\Omega_e} \mathbf{N}^{\mathrm{T}}\mathbf{N}\, \mathrm{d}\Omega$$
$$\mathbf{f}_e^{\text{radiation}} = (\rho_e c_e)^{-1} \int_{\Gamma_e^{\text{out}}} \mathbf{N}^{\mathrm{T}}\mathbf{N}\, \mathrm{d}\Gamma^{\text{out}} \tag{6}$$

where the number of elements is NE and the matrix and vector assembly operators are denoted by $\mathbf{A}_{\mathrm{m}}$ and $\mathbf{A}_{\mathrm{v}}$, respectively. The density and the bulk modulus of the e-th element are denoted by ρ_e and κ_e, respectively. The domain of the e-th element is Ω_e. The boundary for the Sommerfeld boundary condition is defined along Γ_e^{out}. The local stiffness matrix, the local mass matrix and the local damping matrix due to the Sommerfled boundary condition of the e-th element are denoted by $\mathbf{k}_e$, $\mathbf{m}_e$ and $\mathbf{f}_e^{\text{radiation}}$, respectively. The shape function and the strain-displacement matrices are denoted by $\mathbf{N}$ and $\mathbf{B}$, respectively. With out the loss of generality the above formula can be implemented using MATLAB. The present study use the Q4 element for the acoustic simulation in Eqs. (5) and (6).

2.2 Acoustic topology optimization formulation

Compared with the size and shape optimization methods, the topology optimization method allows us to find out an optimal topology to improve the scientific and performance of engineering problem without an initial topology in prior. For the sake of this, the element-wise design variables assigned to each finite element are defined and they are used to interpolate the material properties of the associated governing equation, i.e., the Helmholtz equation, here. In the acoustic topology optimization optimizing the distribution of acoustic pressure, the density and the bulk modulus can be interpolated in order to model psedo rigid body of acoustic domain. In [4,10,11,19,20,26,34] several interpolation schemes have been proposed and this research adopts the following reciprocal interpolation functions of the material properties as follows:

$$\frac{1}{\rho_e} = \frac{1}{\rho_a} + \gamma_e^m \left(\frac{1}{\rho_r} - \frac{1}{\rho_a}\right) \tag{7}$$
$$\frac{1}{\kappa_e} = \frac{1}{\kappa_a} + \gamma_e^m \left(\frac{1}{\kappa_r} - \frac{1}{\kappa_a}\right) \tag{8}$$
$$\rho_r = \rho_a \times 10^7,\ \kappa_r = \kappa_a \times 10^{10} \tag{9}$$

where the density and the bulk modulus of air domain (void domain) are denoted by ρ_a and κ_a, respectively. To model the pseudo rigid domain from an engineering point of view, the pseudo density and the pseudo bulk modulus for rigid domain are denoted by ρ_r and κ_r, respectively. The design variable of the e-th element is denoted by γ_e. For the acoustic topology optimization, the design variables, $\boldsymbol{\gamma}$, are defined at each element. The penalization factor is denoted by m which is set to 5 in the present study. Note that rather than the SIMP (Solid Isotopic material with penalizaiton) is not used. The main reason for using the reciprocal interpolation functions instead of the SIMP method is to reduce the effect of intermediate density elements in acoustic FE analysis. The gray elements in the optimization layout using the SIMP method make errors in acoustic FE analysis. This is because the gray elements have intermediate densities and bulk modulus between the rigid domain and the air domain. On the other hand, when using the reciprocal interpolation function for acoustic topology optimization, the gray elements can be treated like air, thus reducing the error of acoustic FE simulations.

For an optimization formulation, the following optimization problem in Eq. (10) is formulated with the integration of the absolute pressure in the frequency domain from ω_{s} to ω_{e} at the objective domain, Ω_{obj}, inside the analysis domain. The mass constraint is considered to improve the convergence of optimization. Without the mass constraint, many local optima may exist and a small change of the initial condition or the involved parameters causes a dramatic change in the acoustic topology optimization.

$$\begin{aligned} &\underset{\boldsymbol{\gamma}}{\text{Min}}\ \ \Phi = \int_{\omega_{\mathrm{s}}}^{\omega_{\mathrm{e}}} \phi\, \mathrm{d}\boldsymbol{\omega}\ \ \left(\phi = \int_{\Omega_{\text{obj}}} |p|\, \mathrm{d}\Omega\right) \\ &\text{Subject to } \frac{1}{\int_{\Omega_{\mathrm{d}}} 1\, \mathrm{d}\Omega} \int_{\Omega_{\mathrm{d}}} \gamma\, \mathrm{d}\Omega \le \alpha, \\ &\boldsymbol{\gamma} = [\gamma_1, \gamma_2, \ldots, \gamma_{N_e}],\quad \gamma_{\min} \le \boldsymbol{\gamma} \le 1,\quad \gamma_{\min} = 0 \end{aligned} \tag{10}$$

where the objective domain is denoted by Ω_{obj} for the objective function Φ defined as the integration of the absolute value of the pressure on the frequency domain from ω_{s} to ω_{e} and the design domain is denoted by Ω_{d}. The allowed volume ratio is set to α. In the present study, the design variables are normalized from 0 to 1.

The sensitivity of the objective function is computed by considering the conjugate of the acoustic pressure; the sensitivity of the constraint is constant. Although the objective function in Eq. (10) is defined as the integration of the response at a frequency domain, without the loss of generality, the sensitivity analysis for a single frequency is considered. First of all, the Lagrangian considering the forward analysis and the conjugated forward analysis for a frequency of interest ω is formulated as follows:

$$\begin{aligned} &\phi_{\mathrm{L}}(\omega) = \phi(\mathbf{P}, \omega, \gamma) + \boldsymbol{\lambda}_1^{\mathrm{T}} (\mathbf{SP} - \mathbf{F}) + \boldsymbol{\lambda}_2^{\mathrm{T}} \left(\overline{\mathbf{SP}} - \overline{\mathbf{F}}\right) \\ &\text{where } \phi = \int_{\Omega_{\text{obj}}} |p|\, \mathrm{d}\Omega \end{aligned} \tag{11}$$

where the Lagrangian multipliers are $\boldsymbol{\lambda}_1$ and $\boldsymbol{\lambda}_2$. By differentiating the Lagrangian equation as shown in Eq. (12).

$$\frac{\partial \phi_{\mathrm{L}}}{\partial \gamma} = \frac{\partial \phi}{\partial \gamma} + \boldsymbol{\lambda}_1^{\mathrm{T}} \left(\frac{\partial \mathbf{S}}{\partial \gamma}\mathbf{P} + \mathbf{S}\frac{\partial \mathbf{P}}{\partial \gamma} - \frac{\partial \mathbf{F}}{\partial \gamma}\right)$$

$$+\boldsymbol{\lambda}_2^{\mathrm{T}}\left(\frac{\partial\overline{\mathbf{S}}}{\partial\gamma}\overline{\mathbf{P}}+\overline{\mathbf{S}}\frac{\partial\overline{\mathbf{P}}}{\partial\gamma}-\frac{\partial\overline{\mathbf{F}}}{\partial\gamma}\right) \tag{12}$$

The conjugate of the dynamic stiffness matrix is denoted by $\overline{\mathbf{S}}$. In order to eliminate the unknown expression involving $\partial\mathbf{P}/\partial\gamma$ and $\partial\overline{\mathbf{P}}/\partial\gamma$, the following adjoint equations, Eq. (13), can be obtained.

$$\begin{aligned}\mathbf{S}\boldsymbol{\lambda}_1 =&\frac{1}{2}\left(-\frac{\partial\phi}{\partial\mathbf{P}_{\mathrm{Re}}}+i\frac{\partial\phi}{\partial\mathbf{P}_{\mathrm{Im}}}\right),\\ \overline{\mathbf{S}}\boldsymbol{\lambda}_2 =&\frac{1}{2}\left(-\frac{\partial\phi}{\partial\mathbf{P}_{\mathrm{Re}}}-i\frac{\partial\phi}{\partial\mathbf{P}_{\mathrm{Im}}}\right),\\ \boldsymbol{\lambda}_1 \equiv&\overline{\boldsymbol{\lambda}}_2\end{aligned} \tag{13}$$

Note that the real and imaginary parts of the acoustic pressure are denoted by $\mathbf{P}_{\mathrm{Re}}$ and $\mathbf{P}_{\mathrm{Im}}$, respectively. After summarizing the above formula, the final sensitivity analysis can be obtained as follows:

$$\frac{\partial\phi_{\mathrm{L}}}{\partial\gamma}=2\,\mathrm{Re}\left(\boldsymbol{\lambda}_1^{\mathrm{T}}\frac{\partial\mathbf{S}}{\partial\gamma}\mathbf{P}\right) \tag{14}$$

The objective function in Eq. (10) by defined at the frequency domain ($[\omega_s, \omega_e]$), the above sensitivity analysis can be integrated at the frequency domain of interest.

$$\frac{\partial\Phi}{\partial\gamma}=\int_{\omega_{\mathrm{s}}}^{\omega_{\mathrm{e}}}2\,\mathrm{Re}\left(\boldsymbol{\lambda}_1^{\mathrm{T}}\frac{\partial\mathbf{S}}{\partial\gamma}\mathbf{P}\right)\mathrm{d}\boldsymbol{\omega} \tag{15}$$

In the present study, the forward analysis and the sensitivity analysis with and without model order reduction are implemented in MATLAB framework.

2.3 The model order reduction for acoustic optimization

The frequency response functions requiring the consecutive finite element simulations, the acoustic topology requires a huge computational resources. Even a state-of-the art computation, it is still a difficult task to carry out the acoustic topology optimization for a wide range of frequency domain. In order to accelerate the computational procedure, the model order reduction scheme can be applied.

Let us denote the approximated acoustic pressure for the original acoustic press as $\mathbf{P}_{\mathrm{A}}$ and $\mathbf{P}$, respectively. The purpose of the model order reduction is to reduce the degrees of the finite element model by employing the reduction bases, $\boldsymbol{\Psi}$. The individual bases for $\boldsymbol{\Psi}$ are denoted by φ_i, $i = 1, \ldots, n_d$. Thus, the pressure vector is approximated with $\mathbf{P}_{\mathrm{A}} = \boldsymbol{\Psi}\mathbf{Q}$. The frequency dependent reduced vector of order n_d is denoted by $\mathbf{Q}$. By introducing the bases whose number is less than that of the finite element, it is possible to construct the reduced system.

$$\underbrace{\mathbf{P}}_{n\times1}\cong\underbrace{\mathbf{P}_{\mathrm{A}}}_{n\times1}=\underbrace{\boldsymbol{\Psi}}_{n\times n_d}\underbrace{\mathbf{Q}}_{n_d\times1} \tag{16}$$

$$\boldsymbol{\Psi}=[\varphi_1,\ \varphi_2,\ldots,\varphi_{n_d}]\ (n_d\ll n) \tag{17}$$

where the total number of degrees of freedom and the number of the reduced degrees of freedom are denoted by n and n_d, respectively. Thus after multiplying the bases ,$\boldsymbol{\Psi}$, the system matrix can be reduced significantly with a small error as follows:

$$\underbrace{\{\boldsymbol{\Psi}^{\mathrm{T}}\mathbf{S}\boldsymbol{\Psi}\}}_{n_d\times n_d}\underbrace{\mathbf{Q}}_{n_d\times1}=\underbrace{\boldsymbol{\Psi}^{\mathrm{T}}\mathbf{F}}_{n_d\times1} \tag{18}$$

$$\underbrace{\{\boldsymbol{\Psi}^{\mathrm{T}}[\mathbf{K}-\omega^2\mathbf{M}+i\omega\mathbf{F}^{\mathrm{radiation}}]\boldsymbol{\Psi}\}}_{n_d\times n_d}\underbrace{\mathbf{Q}}_{n_d\times1}=\underbrace{\boldsymbol{\Psi}^{\mathrm{T}}\mathbf{F}}_{n_d\times1} \tag{19}$$

As stated, several model order reduction schemes exist. These schemes are classified according to the method of defining the suitable bases for the system of interest, such as mode superposition (MS) method, RV method and QSRV method, etc. (See [1–3,5–9,12–14,18,21–23,27–33,35–37]). The eigenmodes of a system of interest are employed for the Mode Superposition method. The basis of the Krylov subspace composed of external force or system matrix is employed for the Ritz Vector Method. The QSRV method complements the RV method by calculating the bases of dynamic system using the center frequency. All of these model order reduction schemes reduce the degree of freedom for computational efficiency. Among several model order reduction schemes, this research adopts model order reduction with the Ritz vectors. Especially, to improve the accuracy at a wide frequency range, the MQSRV method (Multifrequency Quasi-Static Ritz vector method) is employed. Unlike the other model order reduction schemes, this MOR method computes the reduction bases at *multiple frequencies* of interest as follows:

$$\boldsymbol{\Psi}=\left[\underbrace{\varphi_{1,1}\cdots\varphi_{n_{d,1},1}}_{\text{the 1st domain}}\cdots\underbrace{\varphi_{1,nf}\cdots\varphi_{n_{d,nf},nf}}_{\text{the }(nf)\text{ domain}}\right] \tag{20}$$

where $\varphi_{i,j}$ is the i-th orthonormal basis of the j-th frequency domain. The total number of the divided frequency domain and the number of bases of the j-th frequency domain are denoted by nf and $n_{d,j}$, respectively.

As stable, The quasi-static Ritz method generates the reduction bases at a non-zero center frequency of interest and the multifrequency quasi-static Ritz method generates and combines the bases of the quasi-static Ritz vector method

Algorithm 1 The quasi-static Ritz vector (QSRV) method

1st vector (LU decomposition) : $\varphi_1^* \equiv (\mathbf{K} - \omega_c^2 \mathbf{M} + i\omega_c \mathbf{F}^{\text{radiation}})^{-1}\mathbf{F}$

Normalization with out the mass : $\varphi_1 = \dfrac{1}{\sqrt{\varphi_1^{*\mathrm{T}}\varphi_1^*}}\varphi_1^*$

for $j = 2,\ 3, \cdots,\ n_d$ **do**

j the vector (LU decomposition) :

$\varphi_j^* \equiv (\mathbf{K} - \omega_c^2 \mathbf{M} + i\omega_c \mathbf{F}^{\text{radiation}})^{-1}(\mathbf{M}\varphi_{j-1})$

Orthogonalization without the mass : $\varphi_j^{**} \equiv \varphi_j^* - \sum_{k=1}^{j-1}(\varphi_k^{\mathrm{T}}\varphi_j^*)\varphi_k$

Normalization : $\varphi_j = \dfrac{1}{\sqrt{\varphi_j^{**\mathrm{T}}\varphi_j^{**}}}\varphi_j^{**}$

end for

Algorithm 2 The multifrequency quasi-static Ritz vector (MQSRV) method

1st vector of the 1st frequency domain (LU decomposition) :

$\varphi_1^* \equiv (\mathbf{K} - \omega_{c,1}^2 \mathbf{M} + i\omega_{c,1} \mathbf{F}^{\text{radiation}})^{-1}\mathbf{F}$

Normalization with out the mass : $\varphi_{1,1} = \dfrac{1}{\sqrt{\varphi_1^{*\mathrm{T}}\varphi_1^*}}\varphi_1^*$

for $j = 2,\ 3, \cdots,\ n_{d,1}$ **do**

j th vector of the 1 st frequency domain (LU decomposition) :

$\varphi_j^* \equiv (\mathbf{K} - \omega_{c,1}^2 \mathbf{M} + i\omega_{c,1} \mathbf{F}^{\text{radiation}})^{-1}(\mathbf{M}\varphi_{j-1,1})$

Orthogonalization without the mass : $\varphi_j^{**} \equiv \varphi_j^* - \sum_{k=1}^{j-1}(\varphi_{k,1}^{\mathrm{T}}\varphi_j^*)\varphi_{k,1}$

Normalization without the mass : $\varphi_{j,1} = \dfrac{1}{\sqrt{\varphi_j^{**\mathrm{T}}\varphi_j^{**}}}\varphi_j^{**}$

end for

for $s = 2,\ 3, \cdots,\ nf$ **do**

1st vector of the s th frequency domain (LU decomposition) :

$\varphi_1^* \equiv (\mathbf{K} - \omega_{c,s}^2 \mathbf{M} + i\omega_{c,s} \mathbf{F}^{\text{radiation}})^{-1}\mathbf{F}$

Added orthogonalization : $\varphi_1^{**} \equiv \varphi_1^* - \sum_{p=1}^{s-1}\sum_{k=1}^{n_{d,p}}(\varphi_{k,p}^{\mathrm{T}}\varphi_1^*)\varphi_{k,p}$

for $j = 2,\ 3, \cdots,\ n_{d,s}$ **do**

j th vector of the s th frequency domain (LU decomposition) :

$\varphi_j^* \equiv (\mathbf{K} - \omega_{c,s}^2 \mathbf{M} + i\omega_{c,s} \mathbf{F}^{\text{radiation}})^{-1}(\mathbf{M}\varphi_{j-1,s})$

Added orthogonalization : $\varphi_j^{**} \equiv \varphi_j^* - \sum_{p=1}^{s-1}\sum_{k=1}^{n_{d,p}}(\varphi_{k,p}^{\mathrm{T}}\varphi_j^*)\varphi_{k,p}$

Normalization without the mass : $\varphi_{j,s} = \dfrac{1}{\sqrt{\varphi_j^{***\mathrm{T}}\varphi_j^{***}}}\varphi_j^{**}$

end for

end for

at multiple center frequencies of interest.

$$\omega_{c,j} = \frac{\omega_{j,start} + \omega_{j,end}}{2},\ j = 1, \ldots, nf \tag{21}$$

where the starting frequency, the ending frequency, and the center frequency of the j-th frequency domain are denoted by $\omega_{j,start}$ and $\omega_{j,end}$ and $\omega_{c,j}$, respectively. One of the benefits of the MQSRV method lies in the fact that the improvement of the approximation is achieved at the wider frequencies ranges than the QSRV method specified by the center frequencies. Algorithms 1 and 2 show the algorithms for the QSRV method and the MQSRV method. In these algorithms, the auxiliary variables are denoted by the right upper symbols *, ** or ***.

2.4 Analysis example

In order to validate and show the characteristics of the MQSRV method in acoustics, the two dimensional analysis example in Fig. 1 is analyzed without the loss of generality. Being a simplified two dimensional domain, 1-D the analyt-

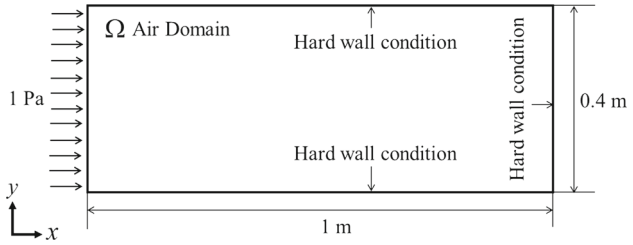

Fig. 1 Analysis example (1000 by 5 discretization, total NE: 5000, total DOF: 6006, frequency domain [1 Hz, 1000 Hz] with Δf = 1 Hz, air speed $c = 343$ m s^{-1}, density: 1.204 kg m^{-3}, bulk modulus: $\rho_a \times c^2$ N m^{-2})

ical pressure can be obtained as follows:

$$1-\text{Dimensional Solution}: \quad P_{\text{Analytical}} = p\left(\cos\left(\frac{\omega}{c}x\right) + \tan\left(\frac{\omega}{c}L\right)\sin\left(\frac{\omega}{c}x\right)\right) \tag{22}$$

With the consideration of the analytical solution in Eq. (22), the finite element simulations with the MQSRV method are carried out in Fig. 1. The three center frequencies are set to 1 Hz, 500 Hz and 1000 Hz and the numbers of the bases at the each center frequencies are increased by one. Thus, the total number of the bases gradually increases from 3 to 12 with 3 interval. Fig. 2a shows the relative error graph with respect to the number of the bases. The relative error in Fig. 2a can be obtained as follows:

$$\text{Relative error} = \log\left(\frac{\int_{\omega_s}^{\omega_e} |\mathbf{P}_{\text{A}} - \mathbf{P}_{\text{Analytical}}| \mathrm{d}\omega}{\int_{\omega_s}^{\omega_e} |\mathbf{P}_{\text{Analytical}}| \mathrm{d}\omega}\right) \tag{23}$$

where the starting frequency and the ending frequency of the analyzed frequency domain is denoted by ω_s and ω_e. Note that by increasing the number of the bases, the discrepancy between the numerical solution and the analytical solution is dramatically decreased as shown in Fig. 2a and b. As the center frequencies are set to 1 Hz, 500 Hz and 1000 Hz, the difference graphs in Fig. 2b illustrate that the discrepancies at the center frequencies are almost zero. The discrepancies at the other frequencies are higher than those near the center frequencies and by increasing the number of the bases, the accuracy is gradually improved.

For the next example, the effects of the bases and the center frequencies are investigated in Fig. 3. The pressure distributions in Fig. 1 are recalculated and the errors are compared by varying the center frequencies with the fixed number of bases at the center frequencies ($n_d = 2$ or $n_d = 4$) in Fig. 3. Note that the approximations at the center frequencies are most accurate at the frequency domain of interest. For example, with the 0 Hz and 50 Hz center frequencies with $n_d = 2$ (case 1), the responses between the frequencies are accurate. By increasing the number of bases to $n_d = 4$ (case 3), it is observed that the prediction is improved. This tendency is also observed at the other frequency domain, i.e., from 300 Hz to 350 Hz (case 2 and case 4). As shown in the case 5 in Fig. 3, it is one of an important characteristics of the MQSRV method for acoustics that the Ritz bases generated at one frequency domain are also improving the accuracy of the approximated solution at another frequency domain. For the example in Fig. 3, the two Ritz bases at 300 Hz and 350 Hz are additionally included to the previous existing Ritz bases at 0 Hz and 50 Hz. Although the Ritz vector at 300 Hz and 350 Hz are included, it is noticed that the response from 0Hz to 50 Hz are improved; compare the responses of case 1, case 3, and case 5. This phenomena is also observed at the frequency domain from 300 Hz, to 350 Hz; compare the responses of cases 2, case 4 and case 5. Then the response at 0 Hz and 50 Hz are improved that suggests that the bases at other center frequencies also can improve the responses.

3 Topology optimization example

To show the efficiency and effectiveness of the MQSRV method for the acoustic topology optimization, this section solves several problems minimizing the acoustic pressure for a wide frequency domain in Eq. (10). The gradient optimizer of the Method of Moving Asymptote is employed [24]. For the initial design, the uniform design variables satisfying the volume constraint are employed. The computation times are computed in the same computational environment CPU: Intel(R) Xeon(R) CPU E5-2699 c3 @2.30GHz(single thread), RAM: 125GB, OS: Red Hat Enterprise Linux release 6.5, MATLAB version: R2020a is used. Fig. 4 shows the optimization procedures of the acoustic topology optimization schemes with and without the model order reduction scheme. The overall procedures are same except the application of the model order reduction scheme in the forward analysis and the sensitivity analysis. One aspect of to be concerned is that the efficiency of the optimization procedure with the model order reduction scheme is dependent on the efficiency of the employed model order reduction scheme. The forward and the sensitivity analysis procedures being mainly accelerated, the comparison of the two procedures in Fig. 4 are made for the sub-procedures, i.e., the forward analysis , the adjoint analysis and the involved other procedures. Note that the responses are approximated solutions but they are accurate enough for an optimizer to find out an optimized design. To assert this, the optimized layouts without the MOR scheme are also obtain and compared.

3.1 Example 1: Rectangular box example

For the first optimization example, the acoustic topology optimization example for the rectangular domain is consid-

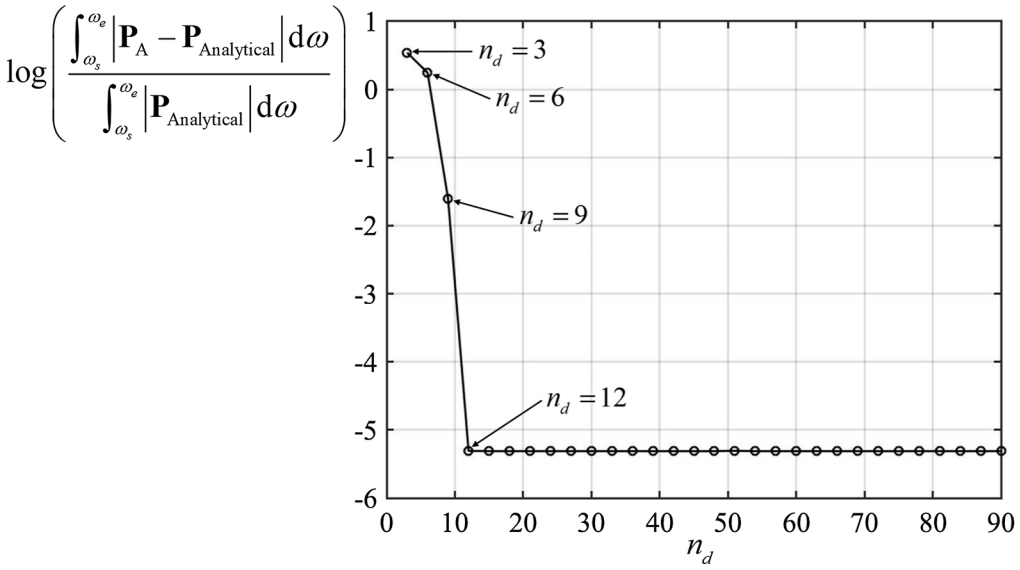

(a)

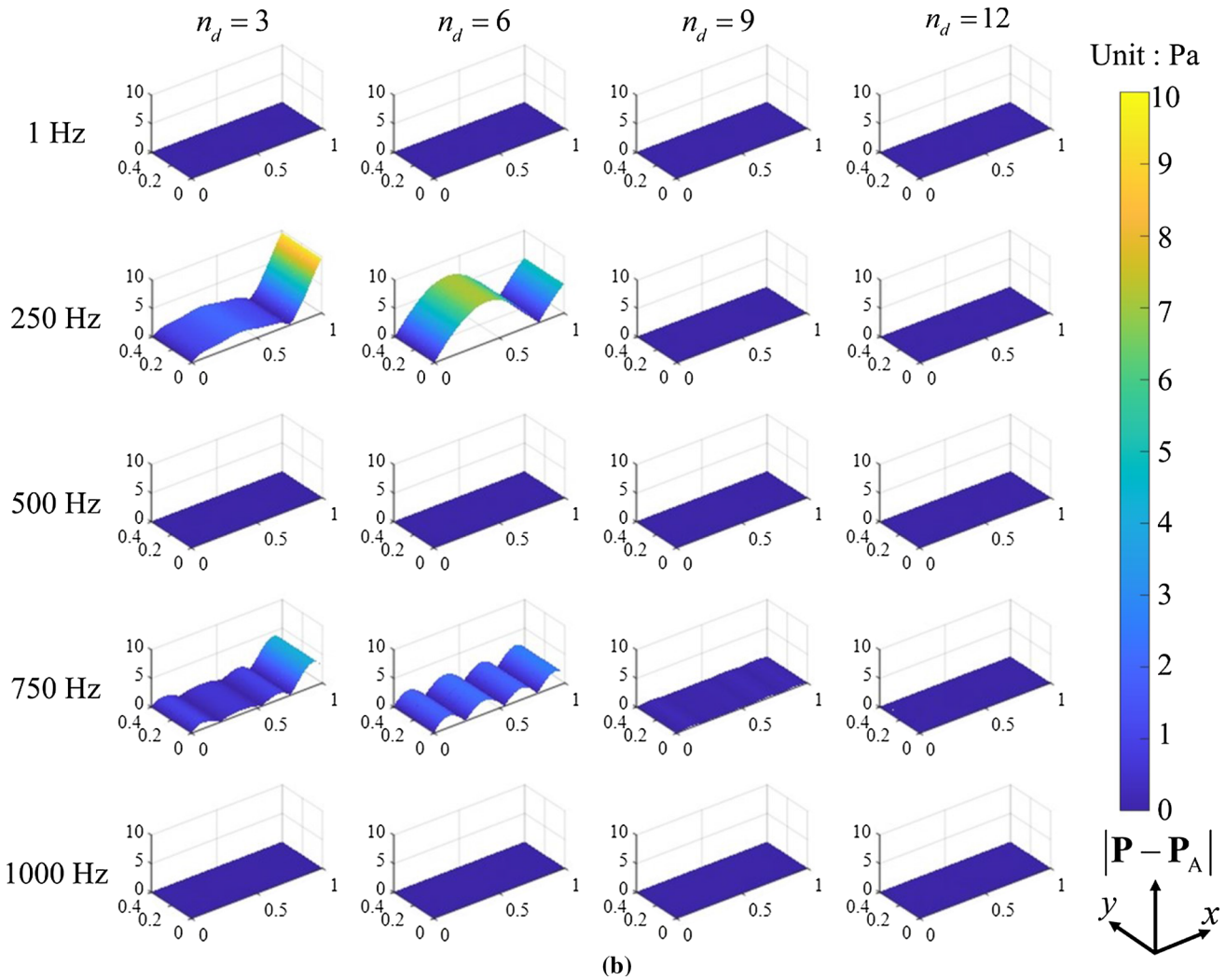

(b)

Fig. 2 Comparison: **a** The relative error graph with respect to the number of the bases; **b** the pressure discrepancies at the five different frequencies (Pressure discrepancies $= |\mathbf{P}_{\mathrm{A}} - \mathbf{P}_{\mathrm{A}}|$)

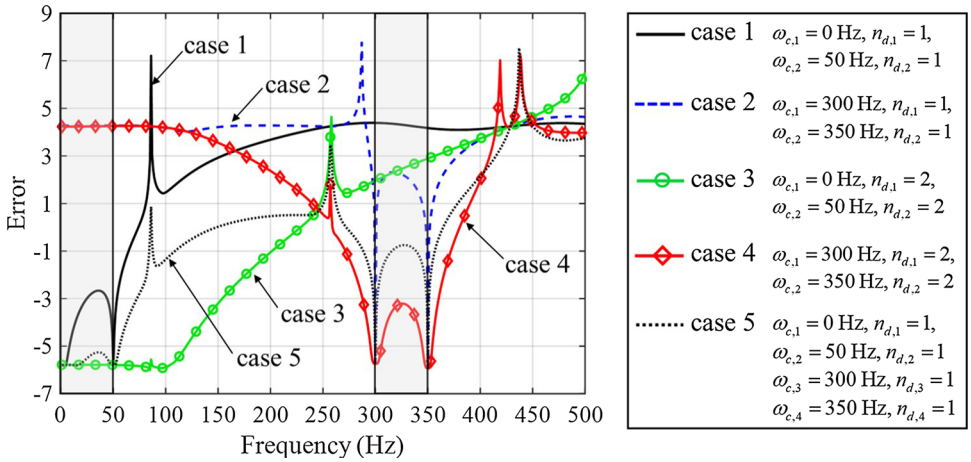

Fig. 3 Error comparisons of the MQSRV method for multiple frequency domains (Error $= \log\left(\frac{|\mathbf{P}-\mathbf{P}_{\text{Analytical}}|}{|\mathbf{P}_{\text{Analytical}}|}\right)$)

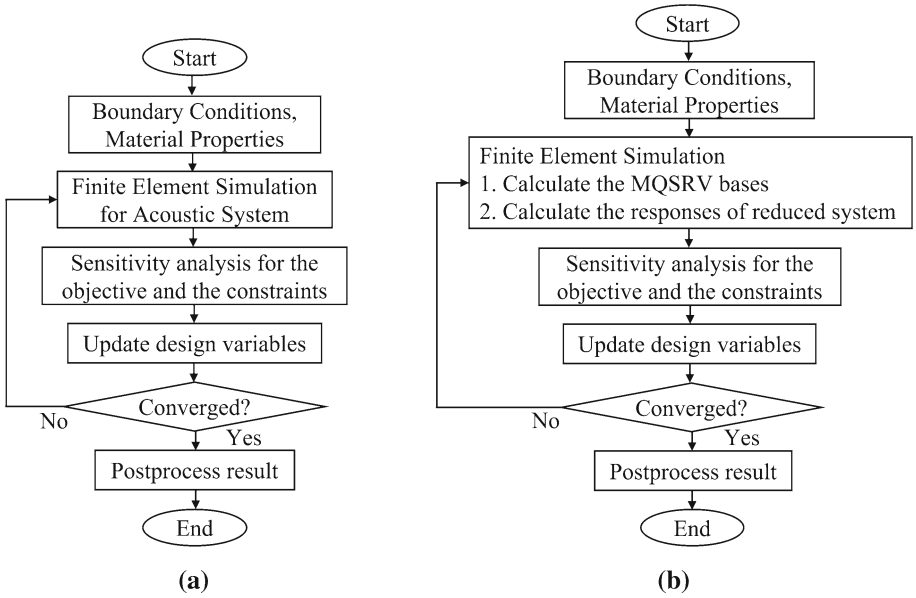

Fig. 4 Optimization process flowcharts. **a** An optimization process without the MOR scheme and **b** an optimization process with the MQSRV scheme

Table 1 Computation of the full order model and the model order reductions for the 1st frequency domain for the example 1

Method	n_d	Φ (N · rad s^{-1}) (FOM / ROM)	CPU times (s) (Speed up [%])		
			Forward	Sensitivity	Total
FOM		74.0628	344.1	338.7	105,634
QSRV	21	84.2741 / 68.2032	6.1 (56.4×10^2)	2.4 (141.1×10^2)	3,457 (30.6×10^2)
MQSRV	3	87.1215 / 126.3155	1.2 (286.0×10^2)	0.3 (1,129.0×10^2)	1,955 (54.0×10^2)
	6	87.0502 / 86.4003	3.2 (107.5×10^2)	0.8 (423.4×10^2)	2,334 (45.3×10^2)
	13	74.9962 / 72.9097	4.8 (71.7×10^2)	1.8 (188.2×10^2)	2,807 (37.6×10^2)
	21	74.0753 / 74.0965	6.1 (56.4×10^2)	2.5 (135.5×10^2)	3,487 (30.4×10^2)

ered in Fig. 5. The hard wall boundary condition is applied at the top and the right sides. The radiation condition is defined along the bottom and left sides. The acoustic field in the objective domain, Ω_{obj}, caused by a point source located at 0.3 m and 0.3 m over the analysis domain is optimized by the topology optimization scheme with the present model order reduction scheme. A solid rectangular domain rendered by black is placed at the center and the off-set design domain rendered by gray in Fig. 5 is assumed. The objective of this optimization is to design the rim of the solid box to minimize the integration of the absolute value of pressure at the objective domain subject to the mass constraint. The inclusion of the mass constraint is for the improvement of the convergence. The rectangular domain is discretized by 120 × 120 quad elements.

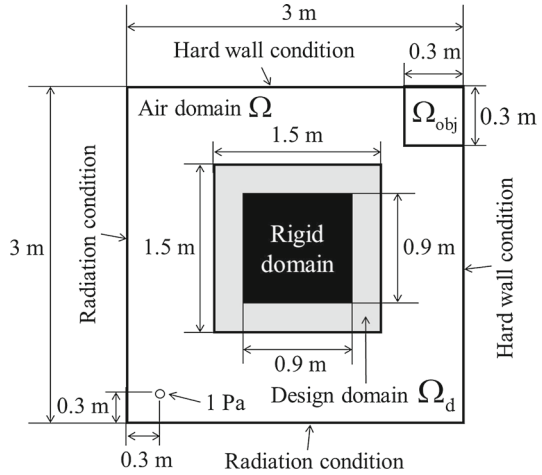

Fig. 5 Rectangular acoustic optimization problem with an internal rigid rectangular domain (Ω_d colored by gray and discretized by 120 × 120 Q4 elements, density of air: 1.204 kg m^{-3}, density of rigid: 1.204 × 10^7 kg m^{-3}, bulk modulus of air: 1.417 × 10^5 N m^{-2}, bulk modulus of rigid: 1.417 × 10^{15} N m^{-2}, air speed c : 343 m s^{-1}, m=5, volume ratio: 25 %)

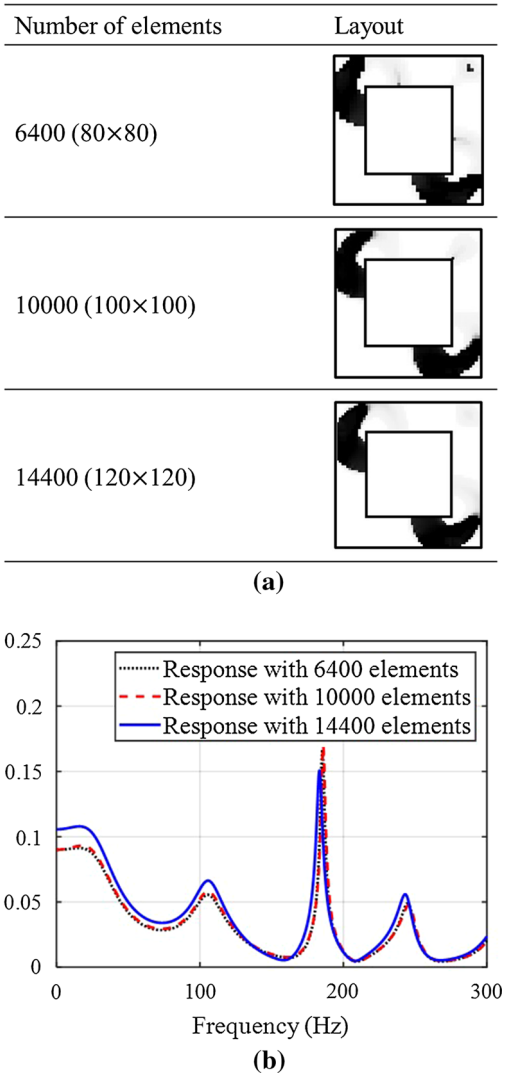

Fig. 6 **a** The optimized layouts by changing the number of elements; **b** the frequency responses of the design with 6400, 10000 and 14400 elements (Discretized by 80 × 80, 100 × 100 and 120 × 120 Q4 elements)

To check the mesh independence of the numerical example, the topology optimization layouts and frequency responses with 3 cases according to the number of elements, i.e. 6400, 10000 and 14400, are shown in Fig. 6. As shown in the figure, similar layouts and the responses are obtained even if the number of elements is changed, thus it is determined that the mesh is independent. To check the effect of intermediate density elements, Fig. 7 compares the frequency responses and layouts of optimized design with and without gray elements. For the layout without gray elements, the design variables of gray elements greater than 0.8 are set to 1 and the rest to 0. As shown in the graph, the two cases obtain similar responses. The topology optimization layouts according to penalization exponent m are shown in Fig. 8. To obtain the layouts with fewer gray elements, m is set to 5. During optimization process the penalization exponent is maintained. Fig. 9 shows the optimization layouts and history with the 100%, 80% and 25% mass constraints. The larger the amount of mass, the smaller the objective values are obtained. This is because the higher the mass amount, the more elements are used to reduce the amplitude of the sound pressure in the objective domain. From on engineering point of view, the optimized layouts with the high mass constraint is difficult to manufacture.

To show the effectiveness of the present approach, the objective responses are computed and accurately integrated with a smaller frequency interval and many matrix inversions are then required per an optimization iteration. Therefore, compared with static optimization problem or dynamic optimization problem with limited matrix inversions, a lot of computational time is inevitably required to carry out the topology optimization. In the present study, to accelerate the analysis and optimization processes, the QSRV method and the MQSRV method are employed [6,12,14,33,35]. Due to the characteristics of the two MOR methods, the QSRV method shows the accurate prediction very near at the single center frequency and the MQSRV method utilizing the combined Ritz vectors at several center frequencies shows the more accurate prediction at the wide frequency domain defined by the multiple center frequencies. The QSRV method sets 150 Hz as a center frequency of the frequency domain of interests for 21 Ritz vectors. For the MQSRV method, without the loss of generality, the 21 center frequencies with the same interval of 15 Hz from 0 Hz to 300 Hz; just one base for each center frequencies. As the number of the Ritz vectors at each frequencies is 1, the total

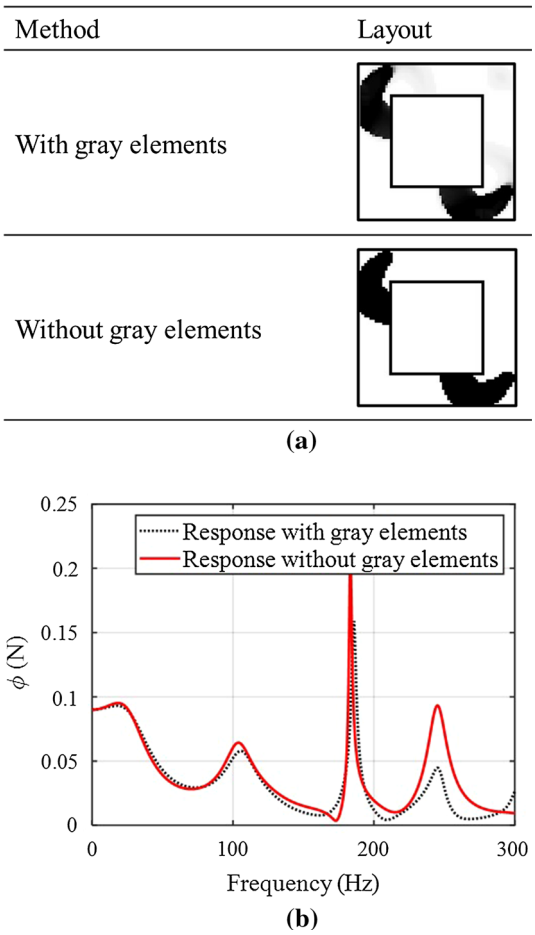

Fig. 7 **a** The optimized layouts with and without intermediate density elements; **b** the responses of the design with and without intermediate densities elements

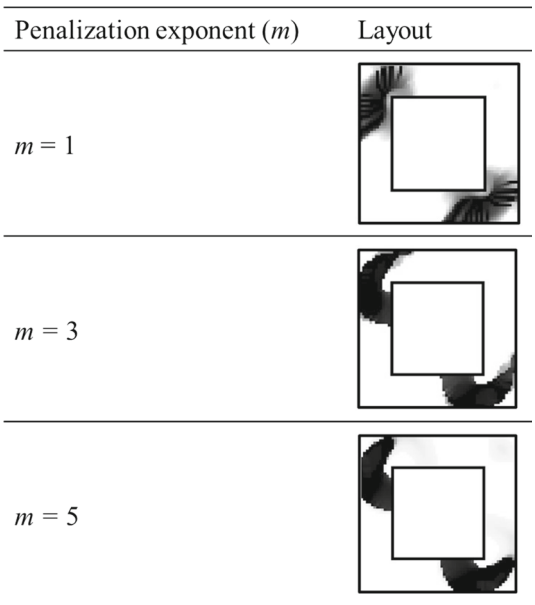

Fig. 8 The optimized layouts according to the penalization exponent, i.e. 1, 3 and 5

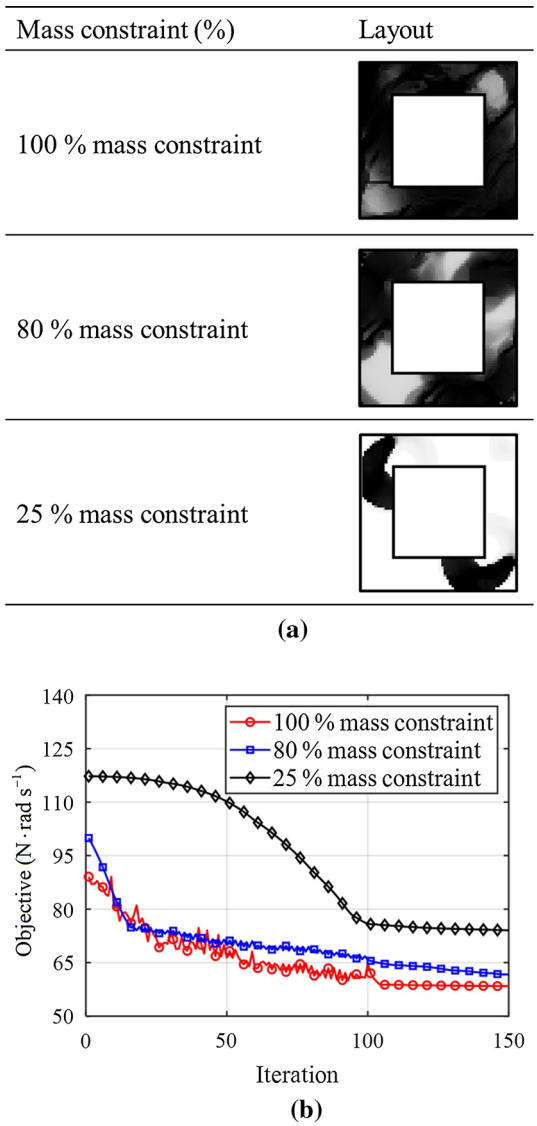

Fig. 9 The optimized layouts according to the mass constraint, i.e. 100%, 80% and 25%

number of the Ritz vectors becomes 21. As the total number of degrees of freedom is 14641, the employed bases are just 0.1434 % (21/14641). The generated Ritz vectors of the MQSRV method are normalized to each other.

Fig. 10a shows the optimized layouts with and without the model order reduction. With the 21 bases, we could obtain the optimized layout similar to the design without the model order reduction. Without the model order reduction, the optimization for 150 iterations process takes 105,634 seconds where it takes 3,457 seconds for the QSRV method (21 bases) and 3,487 seconds for the MQSRV method (21 bases); See Table 1 for more detail. Overall the speed up more than 30 can be achieved. Fig. 11a, b, and c plot the recomputed responses of the standard optimization procedure, the design with the QSRV method, and the design with the MQSRV method.

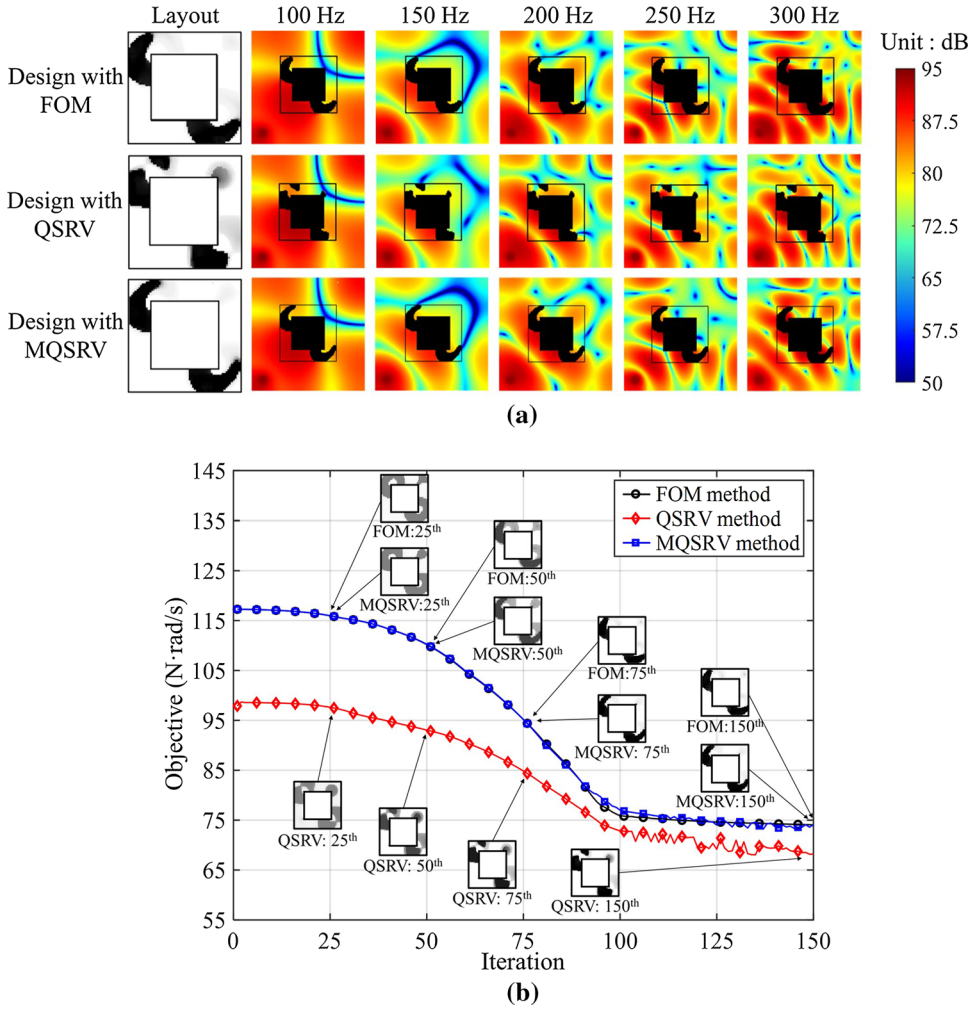

Fig. 10 Example 1: **a** the optimized layouts with the full order model, the QSRV method (n_d= 21 at 150 Hz, 3,457 seconds for 150 iterations) and the MQSRV method (n_d= 21 bases, the center frequencies :[0 Hz: 15 Hz: 300 Hz], 3,487 seconds for 150 iterations) and their pressure distributions; **b** the optimization history (The objective values of the QSRV method are lower due to the erratic computation)

As expected, the response of the QSRV method is accurate at the center frequency, 150 Hz where the MQSRV method shows the accurate response for the frequency domain of interest. Fig. 11c plots the responses of the initial design and the optimized layouts. Fig. 10b shows the optimization histories of the FOM method and the MOR method with 21 the bases. Fig. 12 shows the optimized layouts by changing the number of the bases. With the less bases, the discrepancies between the design of the FOM analysis and the designs of the MQSRV method are observed.

The accuracy of the MQSRV method is dependent of the choice of the center frequencies and the associated number of bases at the center frequencies. These parameters should be chosen considering the characteristics of acoustic simulation of interest. From our computational experiences, it has been observed that by increasing the number of bases, the prediction accuracy is improved. In addition, it is better to increase the number of the center frequencies rather than increasing the number of the bases.

The same problems are solved for the second frequency domain, i.e., from 500 Hz to 800 Hz with the frequency interval 0.25 Hz in Fig. 13. To obtain these designs, 104 Ritz bases are used for the model order reduction scheme, i.e., n_d=104. For the QSRV method, the center frequency is set to 650 Hz which is the middle point of the frequency domain of interest. For the MQSRV method, the evenly distributed 26 center frequencies, i.e., [500 Hz: 12 Hz : 800 Hz], are set and 4 Ritz vectors are computed at each center frequencies ($4 \times 26 = 104$). Note that the optimized layouts and their associated acoustic pressures are similar to each other. In this example, the responses at the frequency domain of interest are evenly minimized as shown in Fig. 13b. The reductions in the computation time and the speed up over the optimization process without the model order reduction are summarized in Table 2. In the present study, the speed up with the present model order reduction is about 15.

In Fig. 14, the two frequency domains, i.e., from 50 Hz to 100 Hz and from 200 Hz to 250 Hz, simultaneously are considered for the objective function. One of the purposes of this example is to illustrate that the bases generated at one frequency domain also can improve the accuracy of the prediction at another frequency domain. For example, the bases

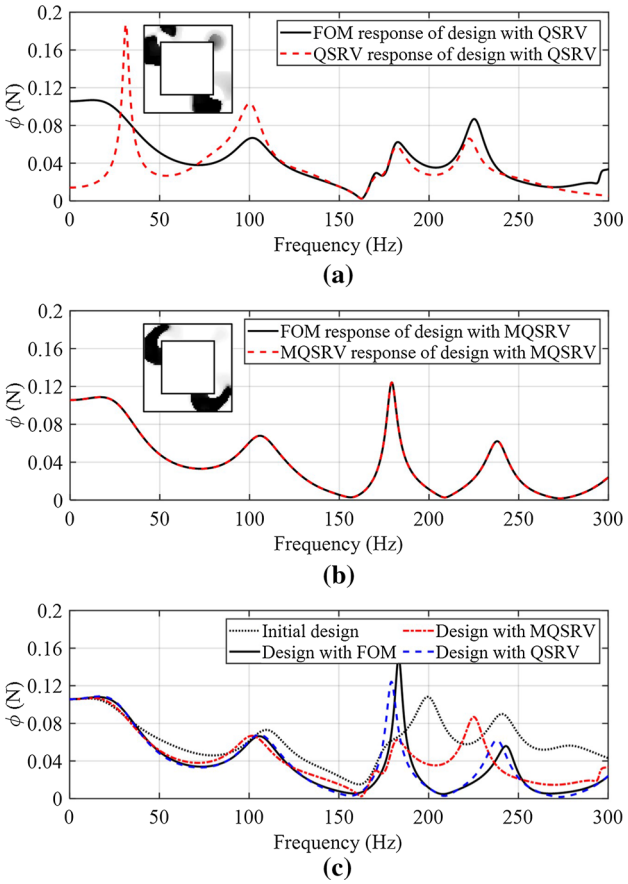

Fig. 11 Response recalculations: **a** the responses of the design with the QSRV method showing the lower accuracy of the QSRV method; **b** the responses of the design with the MQSRV method showing the relatively higher accuracy of the QSRV method; **c** the improvements of the designs (All responses are computed without the MOR scheme)

at the first frequency domain, from 50 Hz to 100 Hz, can be used as the bases for the second frequency domain, from 200 Hz to 250 Hz. Also the bases of the second frequency domain can be used to approximate the dynamic system matrix for the first frequency domain. In this example, 11 bases are generated for the first frequency domain, 50 Hz to 100 Hz with 5 Hz interval, and another 11 bases are also generated for the second frequency domain, 200 Hz to 250 Hz with 5 Hz interval. Thus, the total number of the bases is 22. As shown in Table 3 the similar layout can be obtained. In this example, the speed up over 23 can be achievable.

3.2 Example 2: Pipe design

For the next example, the pipe design problem defined in Fig. 15 is considered. The incoming wave is assumed at the left side and the radiation condition is applied at the right side. The two separated design domains are defined at the upper and the bottom domains. To minimize the integration of the acoustic pressure at the objective domain Ω_{obj}, the optimized structures are obtained in Fig. 16 and in Fig. 17. By investigating the acoustic pressure distributions in Figs. 16 and 17, it turns out that the half spheres cause the resonances like Helmholtz resonators and the acoustic propagation towards the objective domain can be minimized. The responses at Figs. 16b and 17b show that the responses with the MOR scheme are very accurate enough for optimization. With the MQSRV method, the optimized layouts in Fig. 16 can be obtained. As observed in the previous example, the similar layouts can be obtained but with a higher speed up (See Table 4). Depending on the number of the bases, the speed up can be varied. This example shows that the Ritz vector based MOR scheme can be applied for the acoustic problem effectively.

Fig. 17 shows the optimized layout with the two frequency domains of interest. The number of the Ritz vectors for the first frequency domain is 10 when 15 bases are generated for the second frequency domain. The Ritz vectors for the first and second frequency domains are combined together in the MQSRV method. As the bases for one frequency domain also can be utilized for the bases for the another frequency domain in the MQSRV method, the prediction of the MOR scheme is accurate with a smaller error and an optimized layout minimizing the acoustic pressure at the two frequency domains simultaneously can be obtained. Table 5 compares the speed up and the objective values.

Fig. 12 The optimized layouts by changing the number of bases (The objective values are recalculated without the MOR scheme)

Method	FOM	MQSRV			
Layout				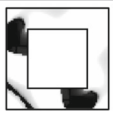	
Center frequencies (Hz)		[0 :150 : 300] $n_d = 3$	[0 : 60 : 300] $n_d = 6$	[0 : 25 : 300] $n_d = 13$	[0 : 15 : 300] $n_d = 21$
Iteration	150	150	150	150	150
Φ (N·rad\s)	74.0628	87.1215	87.0502	74.9982	74.0753
CPU time (s)	105,634	1,955	2,334	2,807	3,487

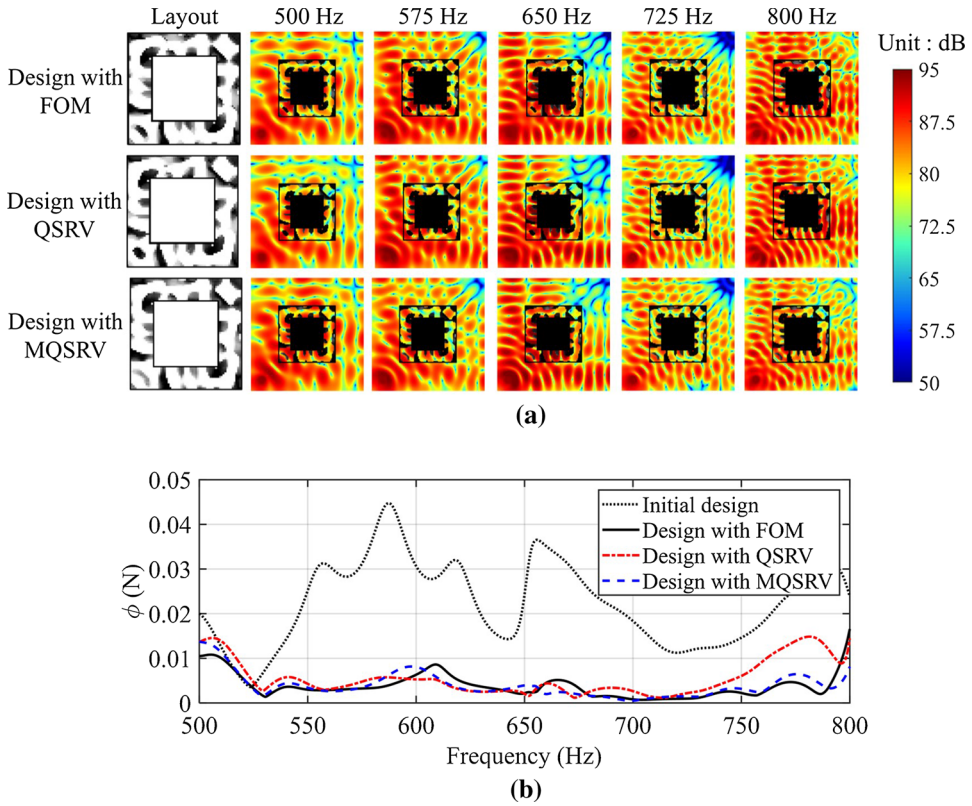

Fig. 13 Optimized layout for the second frequency domain ([500 Hz: 0.25 Hz: 800 Hz]): **a** The optimized layouts with and without the MOR scheme (104 bases for the QSRV method with 650 Hz for the center frequency, 104 bases for the MQSRV method with 104 bases at [500 Hz: 12 Hz: 800 Hz]); **b** the responses of the designs

Table 2 Computation of the full order model and the model order reductions for the 2nd frequency domain for the example 1

Method	n_d	Φ (N · rad s^{-1}) (FOM / ROM)	CPU times (s) (Speed up [%])		
			Forward	Sensitivity	Total
FOM		7.0556	331.4	337.7	153347
QSRV	104	10.3967 / 10.1818	33.4 (9.9×10^2)	17.8 (19.0×10^2)	10018 (15.3×10^2)
MQSRV	104	7.2938 / 7.2938	33.4 (9.9×10^2)	16.8 (20.1×10^2)	10210 (15.0×10^2)

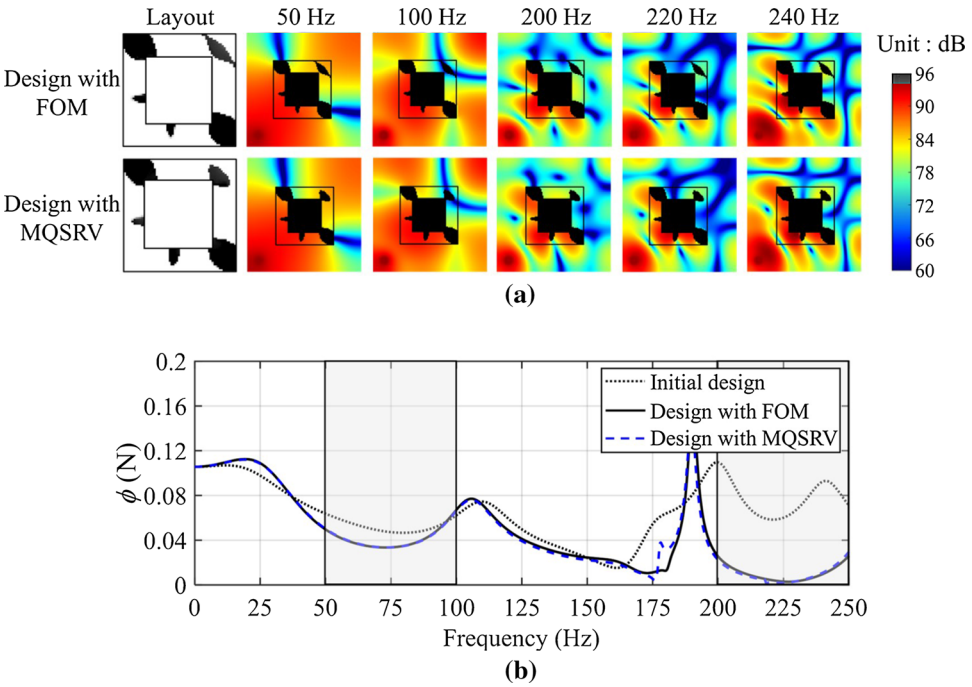

Fig. 14 Optimized layouts with and without the MOR scheme **a** The optimized layouts (The number of basis for the first and second frequency domains are 11 and 11 respectively. One basis at [50 Hz : 5 Hz: 100 Hz] and one basis at [250 Hz: 5 Hz: 300 Hz])

Table 3 Computation of the full order model and the model order reductions for the two frequency domains for the example 1

Method	n_d	Φ (N · rad s^{-1}) (FOM / ROM)	CPU times (s) (Speed up [%]) Forward	Sensitivity	Total
FOM		15.0044	331.8	367.3	101,920
MQSRV	22	14.7270 / 14.7047	7.8 (42.8×10^2)	1.9 (194.0×10^2)	4,336 (23.5×10^2)

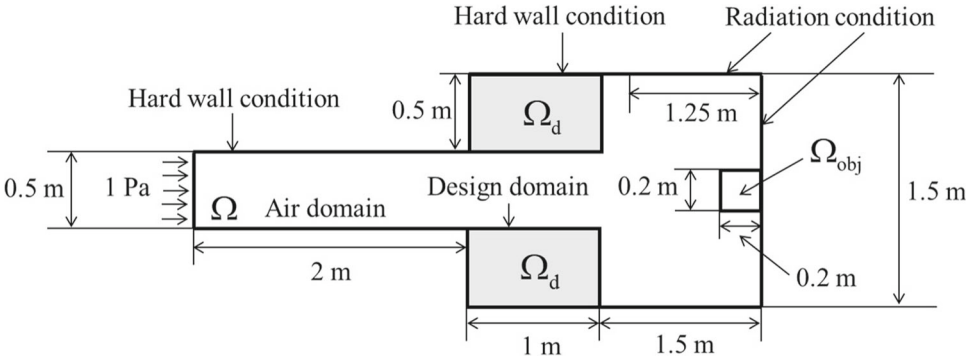

Fig. 15 Pipe design example (The number of degrees of freedom: 7421, the design domain: Ω_d, Frequency domain: $f_s = 150$ Hz $f_e =$ 250 Hz ($\Delta f = 0.05$ Hz), density of air (ρ_a): 1.204 kg m^{-3}, bulk modulus of air (κ_a): $\rho_a \times c^2$ N m^{-2}, density of rigid (ρ_r): $\rho_a \times 10^7$ kg m^{-3}, bulk modulus of rigid (κ_r): $\kappa_a \times 10^{10}$ N m^{-2}, m=5, volume ratio: 25 %)

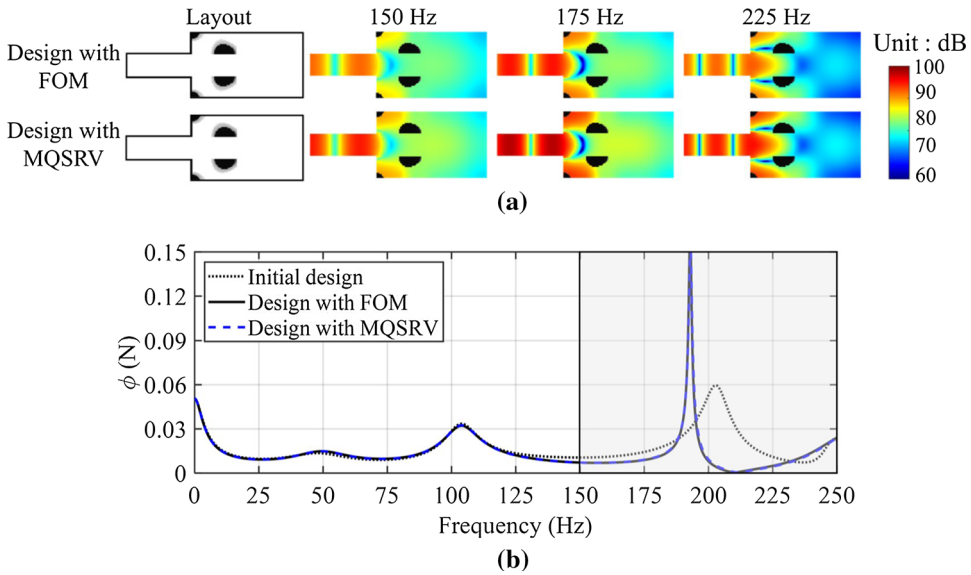

Fig. 16 Optimized layouts with the MQSRV method (Center frequency: [150 Hz:12.5 Hz: 250 Hz], n_d: 27): **a** Optimized layouts and their pressure distributions at several frequencies; **b** the responses of the initial design, the optimized layout without the MOR scheme and the optimized layout with the MQSRV method

3.3 Example 3: Rectangular box example with an enlarged box

For the next example, the optimization problem with the similar design domain discretized by 120 by 120 elements with 14641 degrees of freedom and the boundary conditions is considered in Fig. 18. Compared with the first example, the difference lies in the fact that the center domain is set to the design domain whereas the rim of the domain is set to the design domain in the first example. It is noticed that the local optima issue becomes serious in this enlarged domain for sound source at higher frequency. For a sound source at a higher frequency, a slight change of the design variables may affect acoustic responses significantly and the local optima issue becomes serious. Indeed, in the present example, the lower frequency domain from 50 Hz to 150 Hz is chosen for the frequency domain of interest. The initial design variables are set to 0 for air. Fig. 19 compares the responses of the designs. The acoustic pressure values are generally decreased and the responses of the full order model and the reduced order model are similar. With the present MQSRV method for this example, the speed up around 17 can be achievable that shows the efficiency of the QSRV method and the present MQSRV method (See Table 6). In the QSRV method, 12 bases with 100 Hz for the center frequency are computed and in the QSRV method, the 12 bases are evenly generated; two bases at 50 Hz, 70 Hz, 90 Hz, 110 Hz, 130 Hz and 150 Hz. Fig. 19a show the optimized layouts with the QSRV and the MQSRV method. As stated, the total number of the degrees of freedom in this discretization is 14641. With only 12 bases (0.08 %), it is possible to obtain the similar design of the optimization result with the full order model.

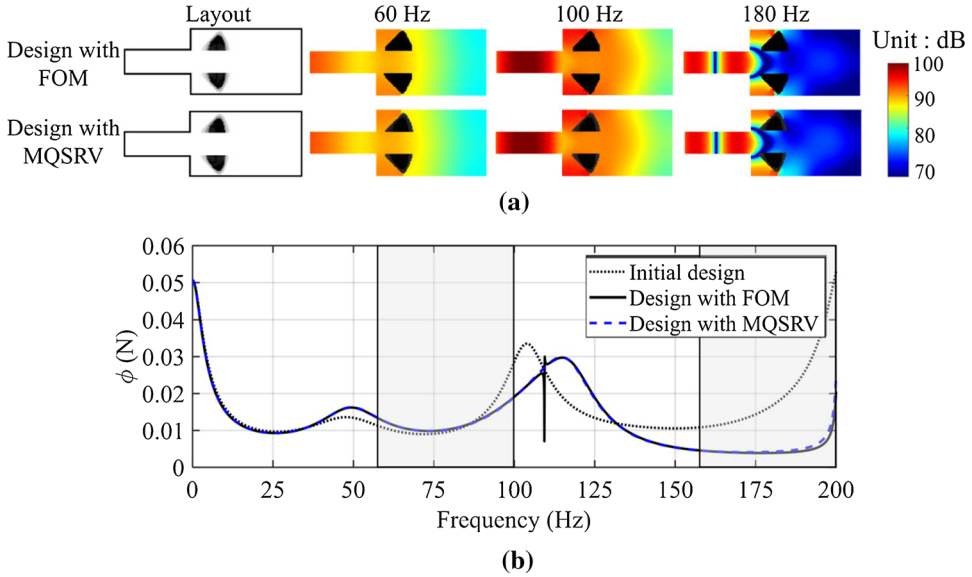

Fig. 17 **a** The optimized layout for the two frequency domains (the first frequency domain: [60 Hz: 0.05 Hz: 100 Hz] and the second frequency domain: [160 Hz: 0.05 Hz: 200 Hz], 10 and 15 bases for the first and second frequency domains, 2 bases at [60 Hz: 10 Hz: 100 Hz] and 3 bases at [160 Hz: 10 Hz: 200 Hz]); **b** the responses of the designs

Table 4 Computation of the full order model and the model order reductions for the frequency domain in Fig. 16

Method	n_d	Φ (N · rad s^{-1}) (FOM / ROM)	CPU times (s) (Speed up [%]) Forward	Sensitivity	Total
FOM		8.0593	89.7	89.9	47,653
MQSRV	27	8.1196 / 8.1159	1.9 (47.2×10^2)	1.6 (56.2×10^2)	3,514 (13.6×10^2)

Table 5 Computation of the full order model and the model order reductions for the two frequency domain in Fig. 17

Method	n_d	Φ (N · rad s^{-1}) (FOM / ROM)	CPU times (s) (Speed up [%]) Forward	Sensitivity	Total
FOM		4.2450	82.6	74.7	37,985
MQSRV	25	4.3658 / 4.3654	1.7(48.6×10^2)	1.5(50.0×10^2)	2464(15.4×10^2)

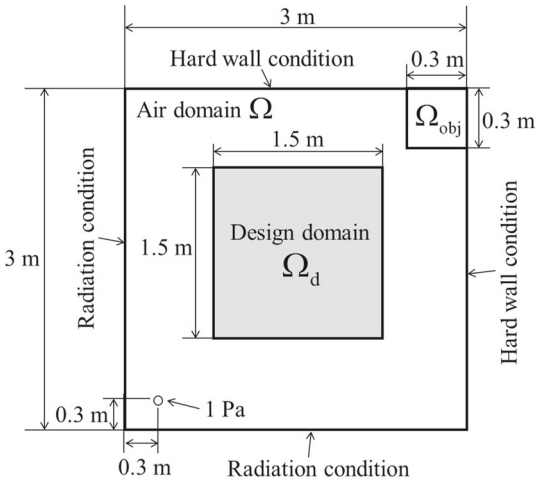

Fig. 18 The third acoustic optimization example problem definition ($f_s = 50$ Hz, $f_e = 150$ Hz, $\Delta f = 0.08$ Hz, the total number of element: 14400 and the number of the degrees of freedom: 14641, density of air(ρ_a): 1.204 kg m^{-3}, bulk modulus of air (κ_a): $\rho_a \times c^2$ N m^{-2}, density of rigid (ρ_r): $\rho_a \times 10^7$ kg m^{-3} , bulk modulus of rigid (κ_r): $\kappa_a \times 10^{10}$ N m^{-2}, m=5, volume ratio: 20 %)

In Fig. 20, the two frequency domains, i.e., from 50 Hz to 100 Hz and from 250 Hz to 300 Hz, simultaneously are considered for the objective function. One of the purposes of this example is to illustrate that the bases generated at one frequency domain also can improve the accuracy of the prediction at another frequency domain. For example, the bases at the first frequency domain, from 50 Hz to 100 Hz, can be used as the bases for the second frequency domain, from 250 Hz to 300 Hz. Also the bases of the second frequency domain can be used to approximate the dynamic system matrix for the first frequency domain. In this example, 11 bases are generated for the first frequency domain, 50 Hz to 100 Hz with 5 Hz interval, and another 22 bases are also generated for the second frequency domain, 250 Hz to 300 Hz with 5 Hz interval. Thus, the total number of the bases is 33. As shown in Table 7 the similar layout can be obtained. In this example, the speed up over 15 can be achievable.

As a final example, Figs. 21 and 22 show the boundary conditions realized the boundary conditions of Fig. 20 in 3 dimension space and an optimized layout in 3 dimension. Fig. 22 is visualized using iso-surface function in MATLAB.

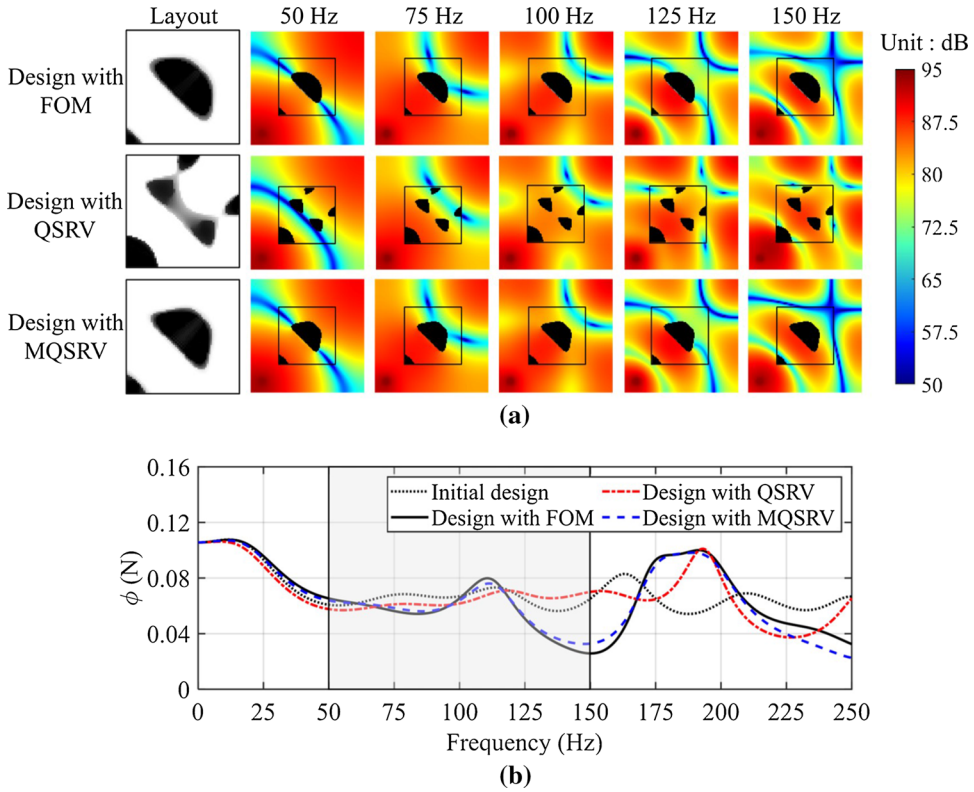

Fig. 19 Optimization results: **a** The layouts comparison with and wihtout the MOR scheme (the QSRV method: 12 bases at 100 Hz for the center frequency, the MQSRV method: 12 bases at the center frequencies (50 Hz, 70 Hz, 90 Hz, 110 Hz, 130 Hz and 150 Hz)); **b** the responses of the designs

Table 6 Computation of the full order model and the model order reductions for the frequency domain in Fig. 19

Method	n_d	Φ (N · rad s^{-1}) (FOM / ROM)	CPU times (s) (Speed up [%])		
			Forward	Sensitivity	Total
FOM		34.9509	206.6	211.3	63,339
QSRV	12	39.9196 / 38.2873	2.5 (82.6×10^2)	1.5 (140.9×10^2)	3,706 (17.1×10^2)
MQSRV	12	35.5083 / 35.4973	2.6 (79.5×10^2)	1.5 (140.9×10^2)	3,759 (16.9×10^2)

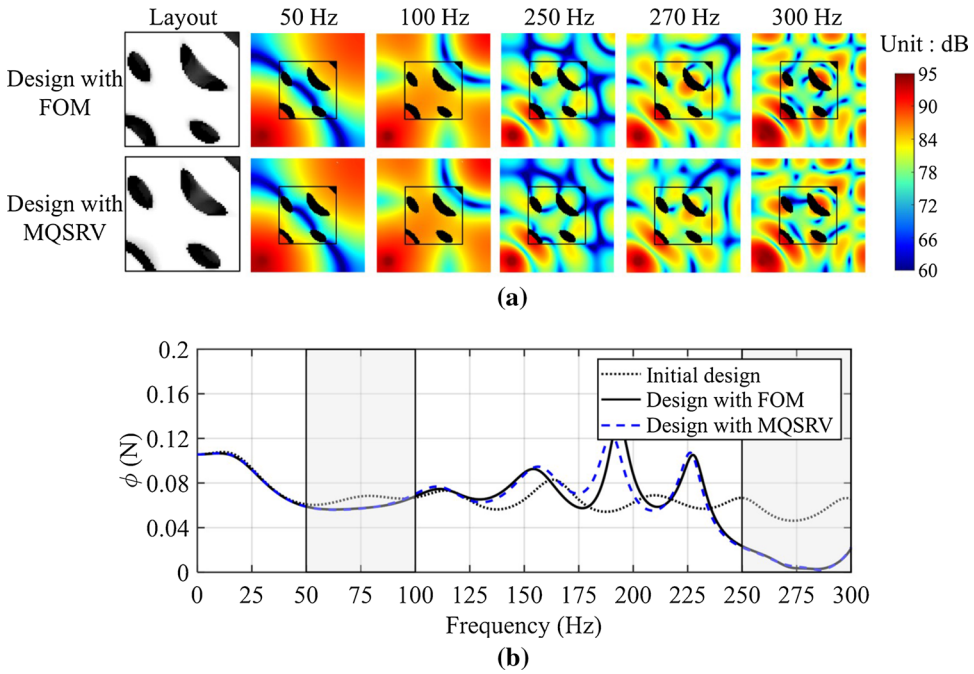

Fig. 20 Optimized layouts with and without the MOR scheme. **a** The optimized layouts (The numbers for the first and second frequency domains are 11 and 22, respectively. One basis at [50 Hz : 5 Hz: 100 Hz], i.e., the number of the bases: $1 \times 11 = 11$ and two bases at [250 Hz: 5 Hz: 300 Hz], i.e., the number of the bases: $2 \times 11 = 22$)

Table 7 Computation of the full order model and the model order reductions for the two frequency domains in Fig. 20

Method	n_d	Φ (N · rad s^{-1}) (FOM / ROM)	CPU times (s) (Speed up [%]) Forward	Sensitivity	Total
FOM		21.5804	192.4	184.1	69,340
MQSRV	33	21.6355 / 21.6122	5.8 (33.2×10^2)	2.3 (80.0×10^2)	4768 (14.5×10^2)

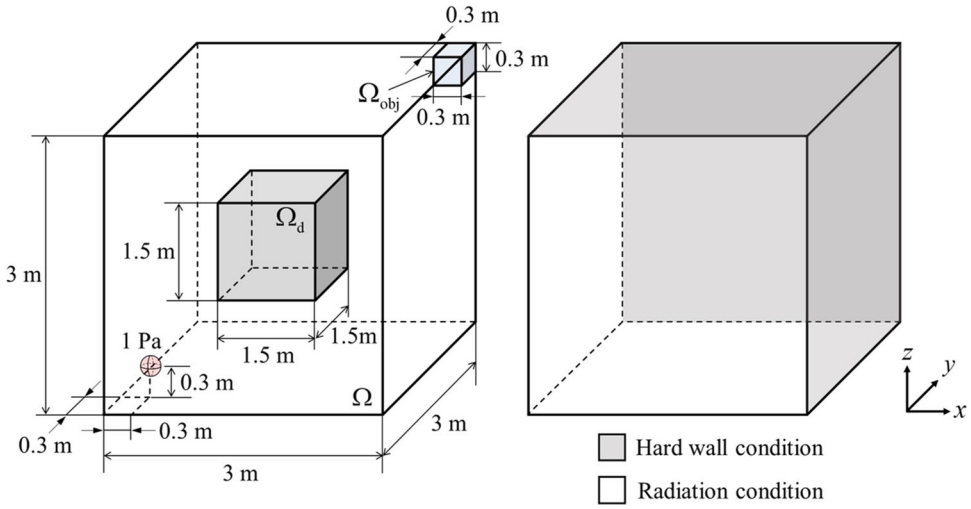

Fig. 21 3D box design design example: (Ω_d colored by gray and discretized by 24 × 24 × 24 Q8 elements, density of air(ρ_a): 1.204 kg/m^3, bulk modulus of air (κ_a): $\rho_a \times c^2$ N/m^2, density of rigid (ρ_r): $\rho_a \times 10^7$ kg/m^3 , bulk modulus of rigid (κ_r): $\kappa_a \times 10^{10}$ N/m^2, air speed c: 343 m/s, m=5, volume ratio: 20 %)

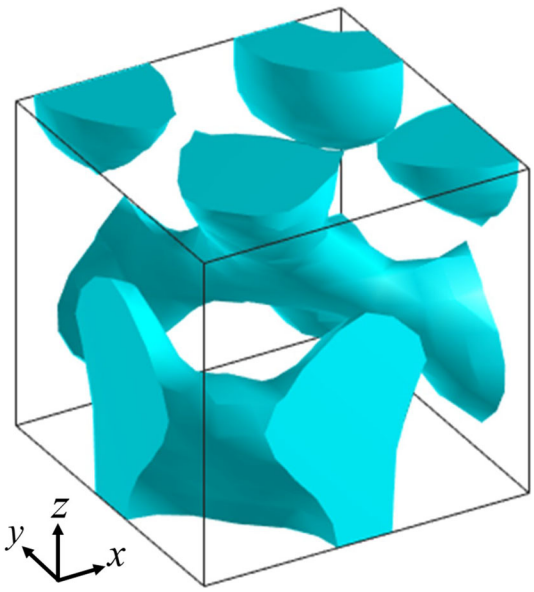

Fig. 22 An 3 dimensional optimized layout with the MQSRV method for the two frequency domains (the first frequency domain: [50 Hz: 0.05 Hz: 100 Hz] and the second frequency domain: [200 Hz: 0.05 Hz: 250 Hz], 11 and 22 bases for the first and second frequency domains, 1 basis at [50 Hz: 0.05 Hz: 100 Hz] and 2 bases at [200 Hz: 0.05 Hz: 250 Hz])

For a clear 3 dimension layout, elements with design variables greater than 0.7 are visualized. The purpose of this example is to investigate the numerical efficiency of the present MQSRV method for 3 dimensional problem. As illustrated, the layouts are similar to each other and as shown in Table 8, the achieved speed up is over 100. This example illustrates that the present MQSRV method is effective in terms of computation and performs well for large-scale acoustic problem.

4 Conclusions

The contributions of the present work are twofold: (a) the development of a new set of the Ritz bases at multiple center frequencies for the improvement of the accuracy of the model order reduction and (b) an efficient acoustic topology optimization based on the model order reduction. The solution of the Helmholtz equation for the acoustic simulation requires a lot of computational time in frequency domain as the dynamic stiffness matrix is dependent on a frequency of interest. Therefore, it is important to accelerate the computation. With the reduction bases computed through the multifrequency quasi-static Ritz vector method, it is possible to reduce the size of the dynamic stiffness matrix significantly and it accelerates the optimization procedure as well as the analysis procedure. In our numerical tests, it is possible to achieve the speed up over 15 times. With an insufficient number of bases, the optimized layouts with the model order reduction are different to the optimized layouts without the model order reduction scheme. Having demonstrated the potential of the model order reduction method for acoustic topology optimization on several design problems, it is possible to explore the application of the Ritz vectors of the

Table 8 Comparison of the full order model and the model order reductions in Fig. 22

Method	n_d	CPU times per iter (s) (Speed up [%])		
		Forward	Sensitivity	Total
FOM		4077.0	4105.7	8182.9
MQSRV	33	50.9 (80.7×10^2)	25.7 (159.8×10^2)	76.7 (106.7×10^2)

MQSRV method for transient problem. Another interesting topic may be to extend the topology optimization approach with the model order reduction scheme for nonlinear structure.

Acknowledgements This work was supported by Korea Institute of Energy Technology Evaluation and Planning (KETEP) grant funded by the Korea government (MOTIE) (20202020800030, Development of Smart Hybrid Envelope Systems for Zero Energy Buildings through Holistic Performance Test and Evaluation Methods and Fields Verifications) and by the National Research Foundation of Korea (NRF) grant funded by the Korea government (MSIT) (No. 2018R1A5A7025522).

Author Contributions These authors contributed equally to this study. Conceptualization: [Gil Ho Yoon], Methodology: [Gil Ho Yoon], Validation, Resources: [Gil Ho Yoon], Writing - Review & Editing: [Gil Ho Yoon], Supervision: [Gil Ho Yoon], Project administration: [Gil Ho Yoon], Formal analysis: [Myung Shin], Investigation: [Myung Shin], Writing - Original draft: [Myung Shin], Visualization: [Myung Shin].

Declarations

Conflict of interest The authors declare that they have no known competing financial interests or personal relationships that could have appeared to influence the work reported in this paper. The authors declare the following financial interests/personal relationships which may be considered as potential competing interests.

References

1. Antoulas AC, Sorensen DC, Gugercin S (2000) A survey of model reduction methods for large-scale systems. Report
2. Choi Y, Oxberry G, White D et al (2019) Accelerating Topology Optimization Using Reduced Order Models. Report, Lawrence Livermore National Lab.(LLNL), Livermore, CA (United States)
3. Demo N, Ortali G, Gustin G et al (2021) An efficient computational framework for naval shape design and optimization problems by means of data-driven reduced order modeling techniques. Boll dell'Unione Mat Ital 14(1):211–230
4. Dühring MB, Jensen JS, Sigmund O (2008) Acoustic design by topology optimization. J Sound Vib 317(3–5):557–575
5. Gordon RW, Hollkamp JJ (2011) Reduced-order models for acoustic response prediction. Report, AIR FORCE RESEARCH LAB WRIGHT-PATTERSON AFB OH AIR VEHICLES DIRECTORATE
6. Gu J, Ma ZD, Hulbert GM (2000) A new load-dependent Ritz vector method for structural dynamics analyses: quasi-static Ritz vectors. Finite Elem Anal Des 36(3–4):261–278
7. Guyan RJ (1965) Reduction of stiffness and mass matrices. AIAA J 3(2):380
8. Han JS, Rudnyi EB, Korvink JG (2005) Efficient optimization of transient dynamic problems in MEMS devices using model order reduction. J Micromech Microeng 15(4):822
9. Heres PJ (2005) Robust and efficient Krylov subspace methods for model order reduction
10. Hu J, Yao S, Huang X (2020) Topology optimization of dynamic acoustic-mechanical structures using the ersatz material model. Comput Methods Appl Mech Eng 372(113):387
11. Kim KH, Yoon GH (2015) Optimal rigid and porous material distributions for noise barrier by acoustic topology optimization. J Sound Vib 339:123–142
12. Koh HS, Kim JH, Yoon GH (2020) Efficient topology optimization of multicomponent structure using substructuring-based model order reduction method. Comput Struct 228(106):146
13. Lee SH, Huang TY, Wu RB (2005) Fast waveguide eigenanalysis by wide-band finite-element model-order reduction. IEEE Trans Microw Theory Tech 53(8):2552–2558
14. Li Q, Sigmund O, Jensen JS et al (2021) Reduced-order methods for dynamic problems in topology optimization: A comparative study. Comput Methods Appl Mech Eng 387(114):149
15. Liu S, Li Q, Liu J et al (2018) A realization method for transforming a topology optimization design into additive manufacturing structures. Engineering 4(2):277–285
16. Ma ZD, Kikuchi N, Hagiwara I (1993) Structural topology and shape optimization for a frequency response problem. Comput Mech 13(3):157–174
17. Ma ZD, Kikuchi N, Cheng HC, et al (1995) Topological optimization technique for free vibration problems
18. Nguyen C, Zhuang X, Chamoin L et al (2020) Three-dimensional topology optimization of auxetic metamaterial using isogeometric analysis and model order reduction. Comput Methods Appl Mech Eng 371(113):306
19. Park GJ, Kang BS (2005) An overview of optimization of structures subjected to transient loads. Trans Korean Soc Mech Eng A 29(3):369–386
20. Pedersen NL (2000) Maximization of eigenvalues using topology optimization. Struct Multidiscip Optim 20(1):2–11
21. Remis RF (2010) An efficient model-order reduction approach to low-frequency transmission line modeling. Progress In Electromagnetics Research 101:139–155
22. Ricles J, Leger P (1993) Use of load-dependent vectors for dynamic analysis of large space structures. Commun Numer Methods Eng 9(11):897–908
23. Song Z, Su D, Duval F et al (2011) Model order reduction for PEEC modeling based on moment matching. Progress In Electromagnetics Research 114:285–299
24. Svanberg K (1987) The method of moving asymptotes-a new method for structural optimization. Int J Numer Meth Eng 24(2):359–373
25. Tango S, Azegami H (2022) Acceleration of shape optimization analysis using model order reduction by Karhunen-Loéve expansion. Jpn J Ind Appl Math 39(1):385–401
26. Tcherniak D (2002) Topology optimization of resonating structures using SIMP method. Int J Numer Meth Eng 54(11):1605–1622
27. Wilson EL (1985) A new method of dynamic analysis for linear and nonlinear systems. Finite Elem Anal Des 1(1):21–23

28. Wilson EL, Yuan M, Dickens JM (1982) Dynamic analysis by direct superposition of Ritz vectors. Earthq Eng Dyn, Struct 10(6):813–821
29. Wittig T, Schuhmann R, Weiland T (2006) Model order reduction for large systems in computational electromagnetics. Linear Algebra Appl 415(2–3):499–530
30. Xia L, Breitkopf P (2014) A reduced multiscale model for nonlinear structural topology optimization. Comput Methods Appl Mech Eng 280:117–134
31. Yao M (1996) Nonlinear structural dynamic finite element analysis using Ritz vector reduced basis method. Shock Vib 3(4):259–268
32. Yoon GH (2010) Structural topology optimization for frequency response problem using model reduction schemes. Comput Methods Appl Mech Eng 199(25–28):1744–1763
33. Yoon GH (2012) Toward a multifrequency quasi-static Ritz vector method for frequency-dependent acoustic system application. Int J Numer Meth Eng 89(11):1451–1470
34. Yoon GH, Jensen JS, Sigmund O (2007) Topology optimization of acoustic-structure interaction problems using a mixed finite element formulation. Int J Numer Meth Eng 70(9):1049–1075
35. Yoon Gil Ho, Kim Jun Hwan, Jung Kwang Ok, Jung Jae Won (2015) Transient quasi-static Ritz vector (TQSRV) method by Krylov subspaces and eigenvectors for efficient contact dynamic finite element simulation. Appl Math Model 39(9):2740–2762
36. Yue Y, Meerbergen K (2013) Accelerating optimization of parametric linear systems by model order reduction. SIAM J Optim 23(2):1344–1370
37. Zhao J, Wang C (2016) Dynamic response topology optimization in the time domain using model reduction method. Struct Multidiscip Optim 53(1):101–114